CHEMISTRY OF MATERIALS

Article

pubs.acs.org/cm

Synthesis of Nonspherical Mesoporous Silica Ellipsoids with Tunable Aspect Ratios for Magnetic Assisted Assembly and Gene Delivery

Shaodian Shen,*[,†] Tao Gu,[‡] Dongsen Mao,[†] Xiuzhen Xiao,[†] Pei Yuan,[§] Meihua Yu,[§] Liyang Xia,[†] Qiong Ji,[†] Liang Meng,[†] Wei Song,[†] Chengzhong Yu,*[,§] and Guanzhong Lu*[,†]

[†]Research Institute of Applied Catalysis, School of Chemical and Environmental Engineering, Shanghai Institute of Technology, Shanghai, 200235, P. R.China

[‡]Ruiqing New Energy Technology Co. Ltd. Hi-Tech Area, 209 Zhuyuan Road, Suzhou 215101, P. R.China

[§]ARC Centre of Excellence for Functional Nanomaterials and Australian Institute for Bioengineering and Nanotechnology, The University of Queensland, Brisbane, QLD 4072, Australia

Supporting Information

ABSTRACT: Despite the extensive application of ellipsoidal micro-/nanoparticles, the synthesis of shape anisotropic ellipsoids is rare because of the minimization of surface free energy that favors simple spherical shape rather than complex nonspherical shape. We present the synthesis of silica ellipsoids with hexagonal mesostructure via the organic−inorganic cooperative assembly in the presence of cosolvents (KCl and ethanol). The aspect ratio of ellipsoids can be tuned systematically by controlling the concentration of ethanol. Transmission electron microscopy (TEM) shows that the ellipsoid possesses one-dimensional (1-D) pore channels parallel to the major axis, and the electron tomography (ET) technique shows that the ellipsoid has indeed hexagonal prism morphology in the middle and ellipsoidal morphology at two tips. A mechanism for the formation of mesoporous silica ellipsoids has been proposed. Importantly, magnetite/silica composite ellipsoids were prepared through a nanocasting route and can be used as building blocks to organize into ordered arrays in response to an external magnetic field. In addition, after functionalized with amino-groups, the amino-modified anisotropic magnetite/silica ellipsoids can be further used as carriers for delivering oligo-DNA-Cy3 into tumor cells, showing potential in directed self-assembly and drug/gene delivery.

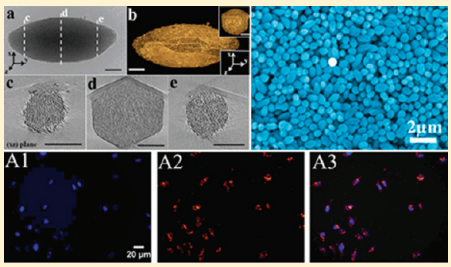

KEYWORDS: *anisotropic particles, cellular internalization, ellipsoids, mesoporous silica, directed self-assembly*

1. INTRDUCTION

Nonspherical micro-/nanoparticles have received considerable attention as compared with their spherical counterparts because of their directed self-assembly[1] for unusual photonic,[2a] electromagnetic,[2b] and rheological properties.[2c−e] Among these nonspherical particles, anisotropic ellipsoidal particles are of particularly interest because their colloidal behavior such as Brownian motion,[3a] maximum packing,[3b] as well as crystal structure[3c] can be tuned systematically by changing the aspect ratio of their axes. Moreover, ellipsoidal particles can be an excellent model system in condensed matter physics[4] and drug delivery vehicle design.[5] For example, Singh et al[6] showed that anisotropic ellipsoids can be organized into both the translational and orientational order through field-guided assembly, leading to new structures that are otherwise unattainable using spherical particles, such ordered structures may have new photonic[7] and mechanical properties.[8] Chen et al[9] described core/shell structured ellipsoids with anisotropic geometry shape for enhanced cellular uptake, showcasing the diverse applications of ellipsoidal shaped structures.

Despite the progress, the synthesis of ellipsoidal particles is, in general, a big challenge because of the minimization of surface free energy that usually favors simple spherical shapes rather than complex nonspherical shapes. Therefore, most synthesis methods currently used have to rely on the anisotropic deformation strategy including high energy ionic irradiation,[10a] chemical ionic etching,[10b] photoinduced deformation,[10c] mechanically stretching,[10d] compressing the presynthesized spherical particles,[10e−g] and microfluidics processing.[10h,i] However, multistep preparation procedures, expensive equipment, and low yield of products limit the application of ellipsoidal particles prepared by these indirect methods. The sol−gel approach provides an alternative route to produce nonspherical particles by carefully controlling the nucleation and growth processes; nevertheless, only a few methods are available for generating ellipsoidal particles.[11] Therefore, it is important to develop a facile approach to fabricate ellipsoidal particles with inexpensive equipment and high yields.

Polymeric surfactants can spontaneously organize into spherical micelles and further transfer to nonspherical rod-like shapes in the presence of ethanol and KCl.[12] We hypothesize that by adding both ethanol and KCl into the surfactant

Received: November 17, 2011
Published: December 4, 2011

dx.doi.org/10.1021/cm203434k | *Chem. Mater.* 2012, 24, 230−235

templating system, mesostructured silica/surfactant composites with nonspherical ellipsoidal morphology can be cooperatively self-assembled.[13] In this work, for the first time, we report the successful synthesis of mesoporous silica ellipsoids using a triblock copolymer EO20PO70EO20 (EO is poly(ethylene oxide); PO is poly(propylene oxide), a commercial product known as Pluronic P123) as the template and tetraethyl orthosilicate (TEOS) as the silica precursor, in the presence of additive agents (KCl and ethanol) under acidic medium. The products exhibit an ellipsoidal morphology and have a highly ordered two-dimensional (2-D) hexagonal mesostructure, with pore channels parallel to the major axis of the ellipsoid. Moreover, the aspect ratio (major versus minor axis) of the mesoporous silica ellipsoids can be tuned systematically by controlling the concentration of ethanol. Significantly, magnetic mesoporous ellipsoidal silica particles have been prepared, which can be directly assembled into ordered arrays in response to external magnetic field. Furthermore, after grafting on the silica surface with amine group, the aminated magnetite/silica ellipsoids show excellent cellular uptake performance with potential applications such as siRNA/gene delivery carriers.

2. EXPERIMENTAL SECTION

(1). Synthesis of Mesoporous Silica Ellipsoids. In a typical synthesis process of nonspherical anisotropic mesoporous silica ellipsoids, 1.60 g triblock copolymer Pluronic P123 was added to a mixture of 1.80 g ethanol, 5.60 g KCl, and 60 g 2 M HCl to form a homogenous solution under stirring at 311 K. Then, 2.12 g of TEOS was added to this solution under vigorous stirring. The molar ratio of P123/ethanol/KCl/HCl/H_2O/TEOS is 1:142:272:435:11200:27. After stirring for 5−10 min, the mixture was kept under static condition at 311 K for 24 h, subsequently, it was transferred into an autoclave to be heated and to be kept at 393K for 24 h. Finally, the solid products were collected by filtration, washed with deionized water thoroughly to remove the KCl salt, dried, and calcined at 773 K for 4 h in flowing air. Mesoporous silica with a tunable aspect ratio was further synthesized by changing the amount of ethanol while the other reaction conditions remained the same.

(2). Synthesis of Fe_3O_4/Silica Composite Ellipsoids. 50 mL of $Fe(NO_3)_3$ solution in ethanol with 3.5 g of $Fe(NO_3)_3{\cdot}9H_2O$ was added to 1.25 g of mesoporous silica ellipsoids particles (aspect ratio of 2.26). After stirring slowly for 10 min, the mixture was dried in air to form $Fe(NO_3)_3$/silica composite; the composite was then calcined at 573K for 3 h and reinfiltrated under the same conditions, followed by calcination at 773K for 3 h. Fe_3O_4/silica composite ellipsoids were obtained after being reduced at 573K for 6 h under H_2 atmosphere.

(3). Assembly of Fe_3O_4/Silica Composite Ellipsoids. The assembly of magnetite/silica composite ellipsoids could be realized through slow drying of the composite suspension in the presence of an external magnetic field. Composite ellipsoidal particles (10 mg) were dispersed in 20 mL of ethanol under sonic treatment. A droplet of particle suspension was deposited on a silicon substrate; subsequently, a neodymium bar magnet (3000 G) was placed adjacent to the droplet with the magnetic field directed either parallel or perpendicular to the substrate. After slow drying of the suspension under ambient conditions, the resulting structure was observed using scanning electron microscopy (SEM).

(4). Mesoporous Magnetitie/Silica Ellipsoids Internalized with HeLa Cells. *(a). Amine Group Modification of Fe_3O_4/SiO_2 Particles.* Fe_3O_4/SiO_2 particles were added into a flask containing 40 mL of toluene and refluxed at 107 °C for 2 h; then, 0.5 mL 3-aminopropyltriethoxysilane (APTES) was added and refluxing continued for another 24 h. The final modified materials were obtained by centrifuging and were washed 3 times with toluene.

(b). Oligo-DNA-Cy3 Binding by Electronic Interaction. 10 μL of 5 mg/mL amine-Fe_3O_4/SiO_2 particles was diluted in 90 μL PBS; then, 1 μL of 10nM oligo-DNA-Cy3 was added in the above solution, and was shaken. After that, the mixture was put into a 4 °C refrigerator overnight. The particles were collected by centrifugation and washed twice with PBS to get rid of unbound oligo-DNA-Cy3. Subsequently, the particles binding with DNA were resuspended in culture media DMEM without Fetal Bovine Serum (FBS), which was ready for the following cell uptake test.

As control groups, we used the unmodified Fe_3O_4/SiO_2 particles treated using above method and same amount of naked oligo-DNA-Cy3 (1 μL of 10 nM) in 100 μL of DMEM without FBS, separately.

(c). Cell Uptake Testing. HeLa cells were plated at 1×10^5 cells per well in a 6-well plate at 37 °C and 5% CO_2 and cultured for another 24 h. After that, the medium was replaced with fresh DMEM without FCS, and then, the suspended complexes of oligo-DNA-Cy3 and particles were added to HeLa cells. After incubation for 5 h, HeLa cells were washed twice with PBS, and then, the cells were fixed with 4% paraformaldehyde, and their nuclei were stained with 5−6 drops of 5 μg/mL 4′,6′-diamidino-2-phenylindole (DAPI) in 10% glycerol. The cells were visualized under a confocal microscope.

Materials Characterization. Scanning electron microscopy (SEM) observations were performed on a Hitachi S-3400N scanning electron microscope operated at 15 kV to clarify the surface structure. For SEM observation, the specimen was coated with gold for 2 min to reduce the charging problem. Transmission electron microscopy (TEM) investigations were performed with an FEI Tecnai T12 transmission electron microscope operated at 120 kV and a JEM-2100 transmission electron microscope operated at 200 kV. The cross-sectional TEM specimens were prepared using ultramicrotome (Leica ultracut 63), and the thickness of the section is ca. 20 nm. The acquisition of the tilt series for electron tomography (ET) was performed with an FEI Tecnai F30 transmission electron microscope operating at 300 kV. All TEM images tilted from −60° to +60° were digitally recorded at a given defocus in a bright-field mode. The data processing was performed with IMOD software.[13] Nitrogen adsorption/desorption isotherms were measured at 77 K by using a Micromeritics ASAP Tristar 3000 system. Prior to examination, the samples were degassed at 453K overnight on a vacuum line.

3. RESULTS AND DISCUSSION

Calcined nonspherical silica with a relatively uniform ellipsoidal morphology and high yield can be observed in a representative low-magnification scanning electron microscopy (SEM) image (Figure 1). The ellipsoidal samples in Figure 1 have an average major axis of 1.38 ± 0.15 μm and minor axis of 0.61 ± 0.07 μm (estimated statistically from SEM images of 50 particles) and an aspect ratio of 2.26. The SEM image taken at a higher magnification (Figure 1 inset) of one individual particle reveals that the geometric shape of the nonspherical silica is a typical ellipsoid. In its low-angle X-ray diffraction (XRD) pattern of calcined mesoporous silica ellipsoids with an average aspect ratio of 2.26 is shown in Figure S1 in the Supporting Information. There are three sharp diffraction peaks that can be indexed as (100), (110), and (200) reflection of a highly ordered, two-dimensional hexagonal *p6m* mesostructure,[14] and the cell parameter calculated from d_{100} is 10.8 nm (Table S1 in the Supporting Information).

The conventional transmission electron microscopy (TEM) image also shows an ellipsoidal morphology (Figure 2a); moreover, it is seen that highly organized 1-D pore channels are oriented parallel to the ellipsoidal major axis over the entire ellipsoidal domain. The distance between two adjacent channels is measured to be ∼9.3 nm, corresponding to the d_{100} spacing. To investigate the internal pore architecture of an individual nonspherical mesoporous silica ellipsoid in relation to the external morphology, the electron tomography (ET) technique[15] was performed (Movie S1 in the Supporting Information). For the selected ellipsoid shown in Figure 2a, a

dx.doi.org/10.1021/cm203434k | *Chem. Mater.* 2012, 24, 230−235

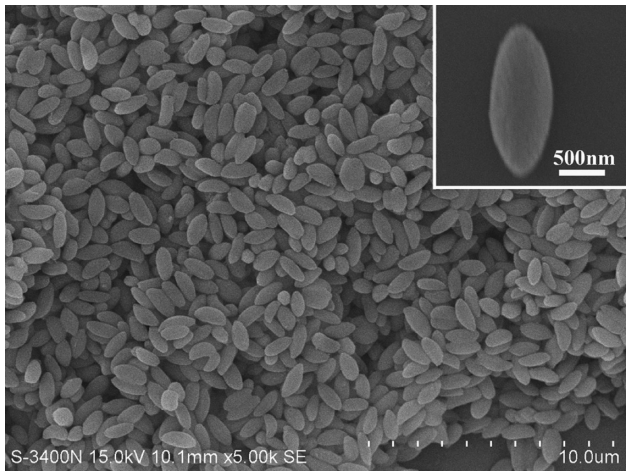

Figure 1. SEM image of the calcined nonspherical mesoporpous silica with ellipsoidal shape; the inset is a high-magnification one.

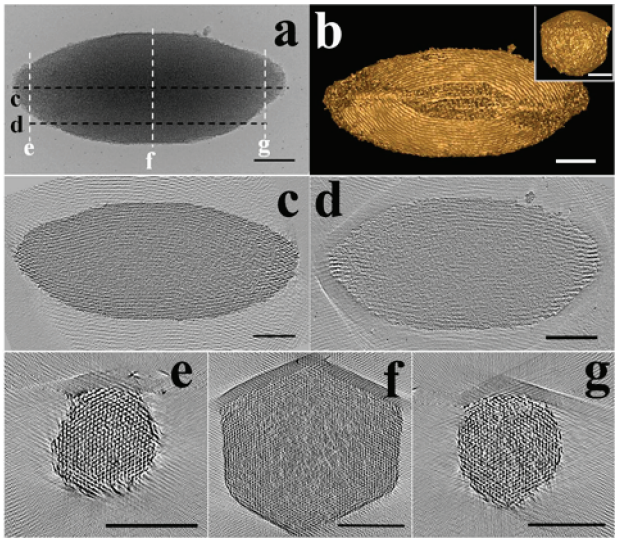

Figure 2. TEM image of (a) typical mesoporous silica ellipsoid and its corresponding 3-D reconstruction, viewing along *z* (b) and *y* (inset of b) axes; (c–e) ultrathin ET tomographic slice images at different positions along the *y*-axis, corresponding to the dashed lines indicated in part a. The Formvar film is located at the top of parts c–e. The scale bar is 200 nm.

series of tilted TEM images ranging from −60° to +60° at an interval of 1° were digitally acquired along the ellipsoidal major axis (*y*- axis, as shown in Figure 2a). Five typical TEM images at the tilt angles of 0, ± 30, and ±60° are shown in Figure S2 in the Supporting Information, showing that the morphology of the particle is similar in the tilt series, while the highly ordered 1-D pore channels can only be observed at given angles (0°, ±60°) because of the nature of the 2-D hexagonal symmetry, in which the d_{100} spacing can only be clearly seen from certain positions with an interval of 60°.

Figure 2b is the surface-rendered reconstruction of the selected ellipsoid with the same view direction as in Figure 2a, which provides the general structural and 3-D morphological information. Interestingly, this particle does not have a smooth surface as expected for a perfect ellipsoid: a sharp edge can be clearly seen along this view direction. Moreover, a hexagonal morphology rather than a round shape can be observed when viewing it along the *y*-axis (inset of Figure 2b). To further

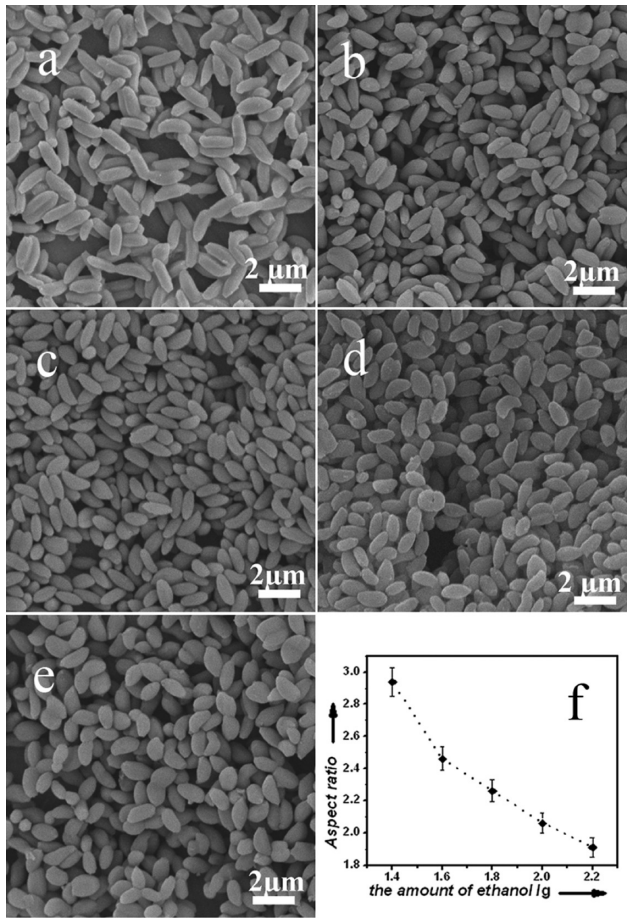

Figure 3. SEM images and plot of nonspherical mesoporous silica ellipsoids with controllable aspect ratio (AR) versus different amounts of ethanol: (a) 1.4 g, AR = 2.94; (b) 1.6 g, AR = 2.46; (c) 1.8 g, AR = 2.26; (d) 2.0 g, AR = 2.02; (e) 2.2 g, AR = 1.91; (f) plot of the change of the aspect ratio of the mesoporous silica ellipsoids with the amount of ethanol added.

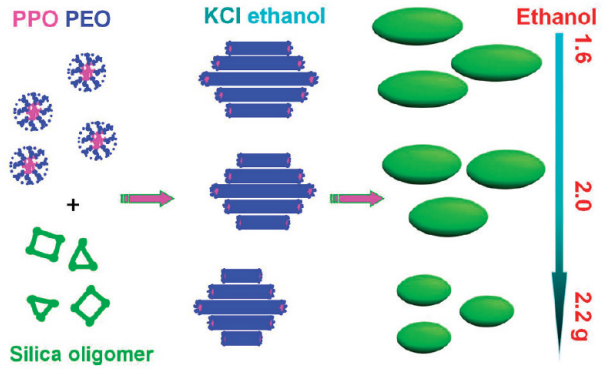

Figure 4. Schematic illustration of the formation of mesoporous silica ellipsoids in the presence of various ethanol amounts.

explore this intriguing structure, the ultrathin tomographic slices on the (*xz*) plane at selected positions along *y*-axis (indicated by dashed lines c, d, and e in Figure 2a) are extracted and shown in parts c–e of Figure 2. The ordered hexagonal mesopore pattern can be clearly seen in all images. It is noted that the shape of the cross section changes from near round at a tip position (dashed line c) to regular hexagon in the middle (dashed line d), and then back to near round shape at another

dx.doi.org/10.1021/cm203434k | *Chem. Mater.* 2012, 24, 230–235

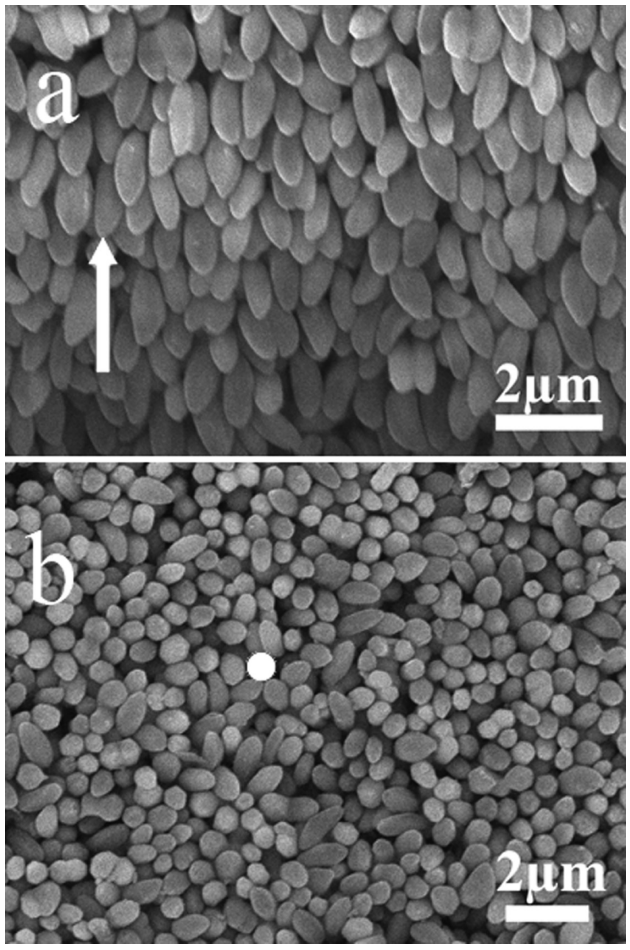

Figure 5. SEM images of the magnetite/silica composite ellipsoids assembled in response to the external magnetic field: (a) ordered multilayer array assembled parallel to the substrate plane and along the magnetic field lines (white arrow); (b) ordered single layer array assembled perpendicular to the substrate and along the magnetic field lines (pointing out-of-paper as indicated by the white dot). Some disorder in the particle orientation can be attributed to the capillary force during solvent evaporation.

tip position (dashed line e), confirming a unique nonperfect ellipsoid morphology. The whole tomogram along the *y*-axis (Movie S2 in the Supporting Information) further shows that the round section is small at one tip and becomes larger as the slice numbers along *y*-axis increase. Meanwhile, the shape changes to hexagon gradually, and the size of the hexagonal section remains nearly constant in the middle of this ellipsoid. Eventually, the hexagonal area becomes smaller, and the section changes back to the round shape near the other tip. Therefore, this ellipsoid has indeed hexagonal prism morphology in the middle and ellipsoidal morphology at two tips. Surprisingly, for the selected hexagonal mesostructured ellipsoid, part b and parts c–e of Figure 2 show that the edge of the prism, rather than a plane, sits on the Formvar film. As a result, the d_{100}, rather than the d_{110}, is observed in Figure 2a. These results also showcase the advantage of the ET technique to characterize unusual structures over conventional SEM or TEM techniques.

The N_2 adsorption–desorption measurement of calcined ellipsoidal silica shows a typical IV isotherm with a clear H1-type hysteresis loop at relatively high pressure (Figure S3 in the Supporting Information). The characteristic parameters of the mesoporous ellipsoidal silica material include a BET surface

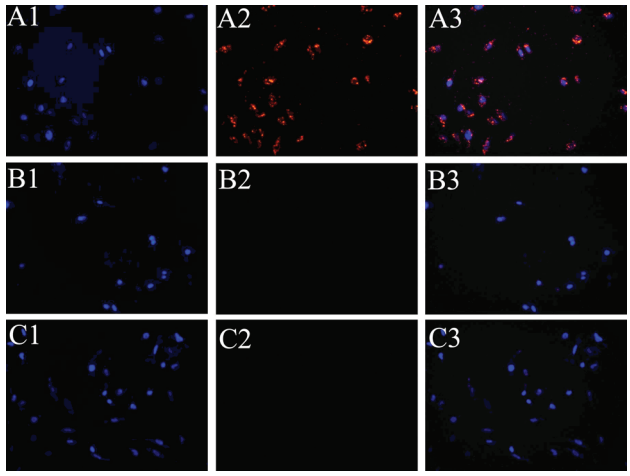

Figure 6. Fluorescence microscopy images of HeLa cells cultivated with (a) amine group modified Fe_3O_4/SiO_2 particles loaded with oligo-DNA-Cy3; (b) Fe_3O_4/SiO_2 particles loaded with oligo-DNA-Cy3 and (c) naked oligo-DNA-Cy3 for 5 h. Blue fluorescence (DAPI stained nucleus) (A1, B1, and C1), red fluorescence (DNA-Cy3) (A2, B2, and C2), and merged fluorescence images (A3, B3, and C3).

area of 773 $m^2 \cdot g^{-1}$, a total pore volume of 1.38 $cm^3 \cdot g^{-1}$, and a narrow pore size distribution centered at 9.4 nm (Figure S3 inset in the Supporting Information).

The additive agents play an important role during the synthesis of nonspherical mesoporous silica ellipsoids. By adding different amounts of ethanol, the aspect ratio of mesoporous silica ellipsoids can be finely tuned. In accordance with a previous work[16] and also as shown in Figure 4 in the Supporting Information, without ethanol or when the ethanol amount is smaller than 1.4 g (see section 2), only rod-like mesoporous silica is generated. When the amount of ethanol is 1.4, 1.6, 1.8, 2.0, and 2.2 g, the aspect ratio of ellipsoid is 2.94, 2.46, 2.26, 2.06, and 1.91, respectively (Figure 3). While the amount of ethanol is higher than 2.2 g in the synthesis solution, mesoporous silica with curled pseudospherical shape can be obtained (Figure S5 in the Supporting Information). The plot shown in Figure 3f illustrates the dependence of the particle aspect ratio on the ethanol concentration, which goes from prolate particles to the ellipsoids with gradually reduced aspect ratio. The mesoporous silica ellipsoids synthesized at different ethanol concentrations are further confirmed by XRD (Figure S6 in the Supporting Information) and nitrogen adsorption–desorption isotherms (Figure S7 in the Supporting Information), and their pore sizes (Supporting Information Figure S8) and other physicochemical parameters are shown in Table S1 in the Supporting Information for comparison. Generally, the surface area decreases with increasing ethanol amounts. Other additives such as propanol and ethylene glycol, as well as K_2SO_4 and KNO_3, were also screened (data not shown), while only using ethanol and KCl as additives can produce the mesoporous ellipsoids.

Many researchers have tried to control the morphology of mesoporous silica by adding cosolvents[17] or cotemplates.[18] In this work, we have shown a first example of shape anisotropic mesoporous ellipsoids with adjustable aspect ratios. Based on our experimental observations, a formation mechanism for mesoporous silica ellipsoids is proposed, as shown in Figure 4. In aqueous solution, $EO_{20}PO_{70}EO_{20}$ tends to form spherical micelles where the hydrophobic PO block is situated in the core and the hydrophilic EO block forms the corona.[19] The

dx.doi.org/10.1021/cm203434k | *Chem. Mater.* 2012, 24, 230–235

addition of a silica precursor and KCl induces the formation of hexagonally patterned rod-like micelles with preferentially equal length.[16] The use of ethanol as the additive may have two roles. First, the ethanol is reported to shorten the length of rod-like micelles.[20] Second, the addition of ethanol delays the colloid phase separation,[21] which favors a spherical morphology due to minimization of surface area (Figure S5 in the Supporting Information). Thus, the ellipsoidal morphology is formed as an intermediate state during the rod-to-sphere transition, and by tuning the amount of ethanol, the aspect ratio of mesoporous silica ellipsoids can be adjusted.

To show the application of anisotropic mesoporous silica ellipsoids in controlled assembly, the mesoporous silica ellipsoids with an aspect ratio of 2.26 were loaded with magnetite by infiltration with $Fe(NO_3)_3$, followed by pyrolysis and reduction. As can be observed in Figure S9 in the Supporting Information, the ellipsoidal morphology is preserved in the magnetite/mesoporous silica ellipsoid composites. The XRD patterns reveal that the composites contain Fe_3O_4 nanoparticles (Figure S10 in the Supporting Information). The TEM image confirms that the Fe_3O_4 is embedded in the confined pore channels (Figure S11 in the Supporting Information). The composite ellipsoids show ferromagnetic properties with a Ms of 8.0 emu/g and a coercivity (Hc) of 225 Oe (Figure S12 in the Supporting Information). The magnetic mesoporous ellipsoids can be further assembled into ordered arrays in response to external magnetic fields. As can be seen in Figure 5, the composite ellipsoids can be organized into nematic-like multilayer and single layer thin film that either parallel or perpendicular to the substrate with their major axes along the applied field direction.[10a,22] To the best of our knowledge, this is the first example of a nonspherical mesoporous material that can be intentionally designed as a building block in directed self-assemblies.

Great efforts[5,23] have been devoted to the exploration of interactions between anisotropic micro-/nanoparticles and cells. To this end, the magnetite/mesoporous silica ellipsoids were further functionalized with amino-groups, using 3-amino-propyltriethoxysilane (APTES), and were used as nanocarriers to test their efficiency to carry oligo-DNA-Cy3 into tumor cells. Figure 6 a1−a3 shows that oligo-DNA-Cy3 can be delivered into HeLa cells using the amine-modified magnetic ellipsoids. In contrast, the oligo-DNA-Cy3 can not be delivered by the unmodified Fe_3O_4/SiO_2 ellipsoids (Figure 6 b1−b3) or in the absence of nanocarriers (i.e., the naked oligo-DNA-Cy3, Figure 6 c1−c3). The results suggest that after proper functionalization, the mesoporous silica ellipsoids can be used as efficient carriers for gene delivery. Considering their large pores and magnetic properties, this material may have excellent potential in targeted delivery and therapy.

4. CONCLUSIONS

In summary, we have demonstrated a direct approach to prepare nonspherical mesoporous silica ellipsoids, the ellipsoids have hexagonally packed pore channels parallel to the major axis, and the aspect ratio of the ellipsoids can be tuned systematically by changing the ethanol concentration. Taking advantage of their porosity, it is possible to fabricate more composite ellipsoids with high refractive index for photonic crystals building blocks. This new type of mesoporous silica ellipsoids may also enable the design of guided self-assembly, multicomponent vehicles for drug delivery or a model system for condensed matter physics.

■ ASSOCIATED CONTENT

Supporting Information

XRD, nitrogen sorption data of nonspherical mesoporous silica ellipsoids in the different amount of ethanol, typical TEM images at different tilt angles, ET Movies, etc. This material is available free of charge via the Internet at http://pubs.acs.org/.

■ AUTHOR INFORMATION

Corresponding Author

*E-mail: shaodian85@yahoo.com.cn; c.yu@uq.edu.au; gzhlu@ecust.edu.cn.

Author Contributions

The manuscript was written through contributions of all authors. All authors have given approval to the final version of the manuscript.

■ ACKNOWLEDGMENTS

We are grateful for financial support from the National Science Foundation of China (20971087/B0101), the National Basic Research Program of China (2010CB732300), Technology Commission of Shanghai Municipality (08ZR1418800) and Education Commission of Shanghai Municipality (12YZ167, J51503), Australian Research Council and the Australian Government's ISL program. Shaodian Shen thanks Prof. Quanshen Zhang for SEM technical support.

■ REFERENCES

(1) (a) Grzelczak, M.; Vermant, J.; Furst, E. M.; Liz-Marzán, L. M. *ACS Nano* **2010**, *4*, 3591. (b) Nie, Z.; Petukhova, A.; Kumacheva, E. *Nat. Nanotechnol.* **2010**, *5*, 15. (c) Yang, S. M.; Kim, S. H.; Lim, J. M.; Yi, G. R. *J. Mater. Chem.* **2008**, *18*, 2177. (d) Glotzer, S. C.; Solomon, M. J. *Nat. Mater.* **2007**, *6*, 557. (e) Xia, Y. N.; Xiong, Y. J.; Lim, B.; Skrabalak, S. E. *Angew. Chem., Int. Ed.* **2008**, *48*, 60. (f) Li, F.; Josephson, D. P.; Stein, A. *Angew. Chem., Int. Ed.* **2011**, *50*, 360. (g) Sau, T. K.; Rogach, A. L.; Jäckel, F.; Klar, T. A.; Feldmann, J. *Adv. Mater.* **2009**, *21*, 1. (h) Feyen, M.; Weidenthaler, C.; Schüth, F.; Lu, A. H. *J. Am. Chem. Soc.* **2010**, *132*, 6791. (i) Park, J.-G.; Forster, J. D.; Dufresne, E. R. *J. Am. Chem. Soc.* **2010**, *132*, 5960. H. (j) Stephanie, L.; Chekesha, M. L. *Small* **2009**, *5* (17), 1957. (k) Kuijk, A.; Blaaderen, A. v.; Imhof, A. *J. Am. Chem. Soc.* **2011**, *133*, 2346. (l) Talapin, D. V.; Lee, J. S.; Kovalenko, M. V.; Shevchenko, E. V. *Chem. Rev.* **2010**, *110*, 389.

(2) (a) Mischenko, M. I.; Hovenier, J. W.; Travis, L. D. *Light Scattering by Nonspherical Particles: Theory, Measurements, Applications*; Academic Press: San Diego, 2000. (b) Guendouz, L.; Ghaly, S. O. S.; Hedjiedj, A. H.; Escanye, J. M.; Canet, D. *Concepts Magn. Reson., Part B* **2008**, *33 B* (1), 9. (c) Madivala, B.; Fransaer, J.; Vermant, J. *Langmuir* **2009**, *25*, 2718. (d) Larson, R. G. *The Structure and Rheology of Complex Fluids*; Oxford University Press: New York, 1998. (e) Lehle, H.; Noruzifar, E.; Oettel, M. *Eur. Phys. J. E: Soft Matter Biol. Phys.* **2008**, *26*, 151.

(3) (a) Han, Y.; Alsayed, A. M.; Nobili, M.; Zhang, J.; Lubensky, T. C.; Yodh, A. G. *Science* **2006**, *314*, 626. (b) Donev, A.; Cisse, I.; Sachs, D.; Variano, E.; Stillinger, F. H.; Connelly, R.; Torquato, S.; Chaikin, P. M. *Science* **2004**, *303*, 990. (c) Radu, M.; Pfleiderer, P.; Schilling, T. *J. Chem. Phys.* **2009**, *131*, 164513.

(4) (a) Letz, M.; Schilling, R.; Latz, A. *Phys. Rev. E* **2000**, *62*, 5173. (b) Chong, S. H.; Götze, W. *Phys. Rev. E* **2002**, *65*, 041503. (c) Vega, C.; Monson, P. A. *J. Chem. Phys.* **1997**, *107*, 2696.

(5) (a) Gratton, S. E. A.; Ropp, P. A.; Pohlhaus, P. D.; Luft, J. C.; Madden, V. J.; Napier, M. E.; DeSimone, J. M. *Proc. Natl. Acad. Sci.*

U.S.A. **2008**, *105*, 11613. (b) Champion, J. A.; Mitragotri, S. *Proc. Natl. Acad. Sci. U.S.A.* **2006**, *103*, 4930.
(6) Singh, J. P.; Lele, P. P.; Nettesheim, F.; Wagner, N. J.; Furst, E. M. *Phys. Rev. E* **2009**, *79*, 050401.
(7) Ding, T.; Song, K.; Clays, K.; Tung, C. H. *Adv. Mater.* **2009**, *21*, 1936.
(8) Mittal, M.; Furst, E. M. *Adv. Funct. Mater.* **2009**, *19*, 3271.
(9) Chen, Y.; Chen, H. R.; Zhang, S.; Chen, F.; Zhang, L.; Zhang, J.; Zhu, M.; Wu, H.; Guo, L.; Feng, J.; Shi, J. *Adv. Funct. Mater.* **2011**, *21*, 270.
(10) (a) Snoeks, E.; Blaaderen, A. V.; Dillen, T. V.; Kats, C. M. V.; Brongersma, M. L.; Polman, A. *Adv. Mater.* **2000**, *12*, 1511. (b) Deng, T.; Cournoyer, J. R.; Schermerhorn, J. H.; Balch, J.; Du, Y.; Blohm, M. L. *J. Am. Chem. Soc.* **2008**, *130*, 14396. (c) Li, Y. B.; He, Y. N.; Tong, X. L.; Wang, X. G. *J. Am. Chem. Soc.* **2005**, *127*, 2402. (d) Jiang, P.; Bertone, J. F.; Colvin, V. L. *Science* **2001**, *291*, 453. (e) Courbaron, A. C.; Cayre, O. J.; Paunov, V. N. *Chem. Commun.* **2007**, 628. (f) Champion, J. A.; Katare, Y. K.; Mitragotri, S. *Proc. Natl. Acad. Sci. U.S.A.* **2007**, *104*, 11901. (g) Hu, Y. X.; Ge, J. P.; Zhang, T. R.; Yin, Y. D. *Adv. Mater.* **2008**, *20*, 4599. (h) Xu, S.; Nie, Z.; Seo, M.; Lewis, P.; Kumacheva, E.; Stone, H. A.; Garstecki, P.; Weibel, D. B.; Gitlin, I.; Whitesides, G. M. *Angew. Chem., Int. Ed.* **2005**, *44*, 724. (i) Dendukuri, D.; Tsoi, K.; Hatton, T. A.; Doyle, P. S. *Langmuir* **2005**, *21*, 2113.
(11) (a) Matijevic, E. *Chem. Mater.* **1993**, *5*, 412. (b) Baek, I. C.; Vithal, M.; Chang, J. A.; Yumb, J. H.; Nazeeruddin, M. K.; Grazel, M.; Chung, Y. C.; Seok, S. I. *Electrochem. Commun.* **2009**, *11*, 909. (c) Yang, Z.; Huck, W. T. S.; Clarke, S. M.; Tajbakhsh, A. R.; Terentjev, E. M. *Nat. Mater.* **2005**, *4*, 486. (d) Sugimoto, T. *Chem. Eng. Technol.* **2003**, *26*, 313.
(12) Denkova, A. G.; Mendes, E.; Coppens, M.-O. *J. Phys. Chem. B* **2008**, *112*, 793.
(13) Kremer, J. R.; Mastronarde, D. N.; McIntosh, J. R. *J. Struct. Biol.* **1996**, *116*, 71.
(14) Wan, Y.; Zhao, D. Y. *Chem. Rev.* **2007**, *107*, 2821.
(15) (a) Yuan, P.; Sun, J. L.; Xu, H. Y.; Zhou, L.; Liu, J. Z.; Zhang, D. L.; Wang, Y. H.; Jack, K. S.; Drennan, J.; Zhao, D. Y.; Lu, G. Q.; Zou, X. D.; Zou, J.; Yu, C. *Chem. Mater.* **2010**, *23*, 229. (b) Miyasaka, K.; Terasaki, O. *Angew. Chem., Int. Ed.* **2010**, *49*, 8867. (c) Sun, J. L.; Zou, X. D. *Dalton Trans.* **2010**, *39*, 8355.
(16) (a) Yu, C. Z.; Fan, J.; Tian, B. Z.; Zhao, D. Y.; Stucky, G. D. *Adv. Mater.* **2002**, *14*, 1742. (b) Sayari, A.; Han, B. H.; Yang, Y. *J. Am. Chem. Soc.* **2004**, *126* (44), 14348.
(17) (a) Polshettiwar, V.; Cha, D.; Zhang, X.; Basset, J. M. *Angew. Chem., Int. Ed.* **2010**, *49*, 9652. (b) Yoo, W. C.; Stein, A. *Chem. Mater.* **2011**, *23*, 1761. (c) Zhao, D. Y.; Sun, J. Y.; Li, Q. Z.; Stucky, G. D. *Chem. Mater.* **2000**, *12* (2), 275. (d) Li, N.; Wang, J. G.; Zhou, H. J.; Sun, P. C.; Chen, T. H. *Chem. Mater.* **2011**, *23* (18), 4241.
(18) (a) Yang, S.; Zhou, X.; Yuan, P.; Yu, M.; Xie, S.; Zou, J.; Lu, G. Q.; Yu, C. *Angew. Chem., Int. Ed.* **2007**, *46*, 8579. (b) Li, N.; Wang, J. G.; Zhou, H. J.; Sun, P. C.; Chen, T. H. *Chem. Mater.* **2011**, *23* (18), 4241.
(19) Wanka, G.; Hoffmann, H.; Ulbricht, W. *Macromolecules* **1994**, *27*, 4145.
(20) Denkova, A. G.; Mendes, E.; Coppens, M.-O. *J. Phys. Chem. B* **2009**, *113*, 989.
(21) Yu, C. Z.; Fan, J.; Tian, B. Z.; Zhao, D. Y. *Chem. Mater.* **2004**, *16*, 889.
(22) Lee, S. H.; Song, Y. I.; Hoseina, D.; Liddell, C. M. *J. Mater. Chem.* **2009**, *19*, 350.
(23) (a) Meng, H.; Yang, S.; Li, Z.; Xia, T.; Chen, J.; Ji, Z.; Zhang, H.; Wang, X.; Lin, S.; Huang, C.; Zhou, Z. H.; Zink, J. I.; Nel, A. E. *ACS Nano* **2011**, *5*, 4434. (b) Huang, X.; Teng, X.; Chen, D.; Tang, F.; He, J. *Biomaterials* **2010**, *31*, 438. (c) Suteewong, T.; Sai, H.; Cohen, R.; Wang, S.; Bradbury, M.; Baird, B.; Gruner, S. M.; Wiesner, U. *J. Am. Chem. Soc.* **2011**, *133*, 172.